Pasteless, Active, Concentric Ring Sensors for Directly Obtained Laplacian Cardiac Electrograms

Chih-Cheng Lu* Peter P. Tarjan[1]

Division of Medical Engineering Research, National Health Research Institute, Taipei, Taiwan, 104, ROC
[1]*Department of Biomedical Engineering, College of Engineering, University of Miami, Coral Gables, FL 33146, USA*

Received 3 October 2002; Accepted 21 November 2002

Abstract

Abnormal propagation paths and velocities characterize cardiac arrhythmias. Conventional surface ECGs provide only global information and tend to smooth the original signal in time, making it difficult to determine the moment of activation (MoA) at a specific point. We developed an active tripolar concentric ring sensor capable of detecting the Laplacian electrogram (LECG) resolution. The signal conditioning amplifiers and their power supply are mounted directly on the back of the sensor. The uniquely designed instrumentation amplifier (IA) provides high input impedance, therefore skin preparations is not necessary. The inherent common mode rejection(CMR) from the tripolar concentric ring sensor and the high common mode rejection ratio (CMRR=117dB) from the IA yield 0.7 μV_{rms} noise level at the output with gain of 1000. The Directly Obtained Laplacian Cardiac Electrogram is obtained in real time without digital signal processing.

***Keywords*:** Laplacian ECG, Concentric ring electrodes, Active sensor

Introduction

There are many different methods to observe the heart rhythm, using either invasive or non-invasive measurement techniques. Einthoven initially developed the recording of the body surface ECG in 1902 [4] and it has become the most common tool for the non-invasive detection of the electrical activity of the heart. The ECG provides global information about the direction, amplitude, and speed of propagation of the depolarization, but the signals do depend on the locations and other features of the electrodes. By using large arrays of electrodes combined with intensive digital signal processing, the direction of propagation and local activation time can be obtained non-invasively and presented graphically [6].

Hjorth [7] first proposed the rectangular finite difference approximation method from a center electrode and four neighboring electrodes on a square to study the Laplacian Electroencephalogram (LEEG). Later, He [6] used that method for the LECG. The finite difference algorithm for LECG involved averaging small differential signals between the center and the corner electrodes. A poor SNR is expected due to quantization errors from digitizing the data. Furthermore, substantial differences were noted when the rectangular sensor array was rotated by 45° [5].

* Corresponding author: Chih-Cheng Lu
Tel: +886-2-26524161 ; Fax: +886-2-26524141
E-mail: clu@nhri.org.tw

Usually, the electrical activity at a specific location in the heart is determined in real time by an invasive method. Several leads with multiple sensing electrodes are inserted into the heart via blood vessels to obtain the information of interest from specific sites. This invasive method provides the gold standard for localized information about the propagation of electrical activity, such as the spatial and temporal course of depolarization in the heart. However, spatial resolution is dependent on the movement of the heart with respect to the chest and the biplane imaging system [1]. This procedure is typically performed by an "invasive cardiologist," a highly trained specialist, with complex and expensive instruments (X-ray imaging systems and disposable leads) and a cardiac surgeon to stand by in case a life-threatening complication were to arise.

Our objective was to develop an active concentric ring sensor to acquire high quality LECG signals from the body surface in real-time, without skin preparation.

Methods

Active Sensor

The active sensor consists of two parts: a set of three concentric ring electrodes on a non-conductive substrate, and a signal conditioning amplifier mounted directly on the back of the substrate.

Concentric ring electrode

Fattorusso pioneered the use of concentric ring electrodes,

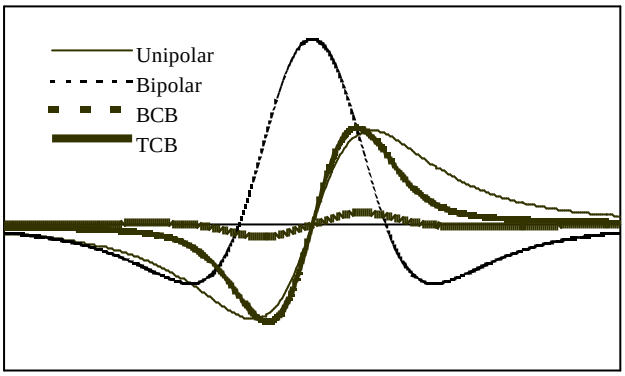

Figure 1. Computer simulation for four different types of sensors.

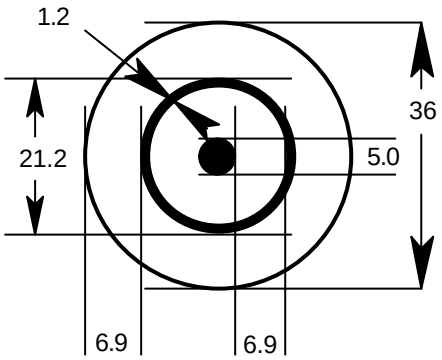

Figure 2. Tripolar concentric ring sensor connected in bipolar configuration as a TCB sensor.

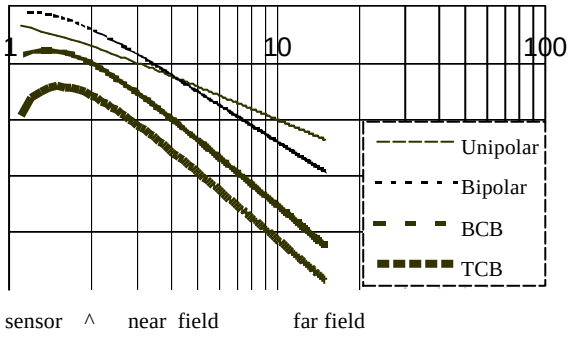

Figure 3. Normalized log-log scale for far-field rejection from the outer limit of each sensor at "1" to far away from the sensors ("100"). Note: the zero crossing of the TCB forces the signal to vanish at the outer ring and rise within the outer ring. Compare with Fig. 1.

or "coaxial electrodes," for recording bioelectric activity, in 1949 [2]. The sensor consisted of a ring conductor and a center dot designed to record the spatial derivative of an electrical signal directly under the concentric sensor. It was used to study myocardial infarcts and arrhythmias related to bundle branch blocks.

Computer simulation of the concentric ring electrode was conducted by Kaufer to optimize the dimensions of the concentric ring sensor [8]. The computer model simulates four different types of sensors with the sensor parallel to the moving direction of the dipole (Fig. 1).

The unipolar sensor is used most commonly to acquire signals. The chest leads, V1 ~ V6, in a standard 12-lead ECG are typical unipolar recordings. Unipolar sensors detect the potential generated by the wavefront, with a roll-off inversely proportional to the square of the distance between the wavefront and the sensor.

Bipolar sensors detect the difference between two unipolar sensors. They enhance localized information by rejecting the far field with the inverse third power of distance between the wavefront and the center of the bipolar sensor.

A bipolar concentric ring "bipolar" (BCB) sensor has a small ring/dot at the center of a concentric ring [3]. The signal is the difference between the two concentric rings. As the wavefront moves directly underneath the sensor, it generates a signal as a function of time that is equivalent to the second spatial derivative of the potential at the body surface that is defined as the LECG. The bipolar ring sensor's far-field rejection is proportional to the inverse fourth power of the distance between the wavefront and the center of the sensor [9]. This is more selective than the sensitivity of the unipolar sensor, which falls off with R^{-2}, and of the bipolar sensor that falls off with R^3. It provides the best far field rejection among these three sensors.

The final sensor modeled in the simulation study was a tripolar concentric ring sensor. It consisted of two concentric rings and a dot at the center (Fig. 2).

This sensor can register three signals: V_o outer ring voltage, V_m middle ring voltage and V_c center dot voltage. The output of the sensor, V_{out}, is the difference between the two voltages sensed by the outer gap and the inner gap:

$$V_{out} = (V_o - V_m) - (V_m - V_c)$$

This tripolar configuration can be simplified by connecting the outer ring to the center dot as a non-inverting input to a differential amplifier while subtracting the inverting input from the middle ring itself. This tripolar concentric ring sensor, configured as a bipolar input, is referred to as the TCB sensor. The TCB sensor has high inherent CMR. The common electrical noise induced in the outer and the inner gap are effectively canceled.

The TCB sensor provides the second spatial derivative as the BCB sensor. We can show this double spatial differentiation mathematically as follows:

$$V_{TCB} = 0.5\,(V_O + V_C) - V_M$$
$$= 0.5\{(V_o - V_m) - (V_m - V_c)\}$$
$$= 0.5\,(\Delta V_{om} - \Delta V_{mc}) \approx d^2V / dx^2$$

where V_{TCB} : output voltage of the TCB sensor;
V_o : outer ring voltage;
V_m : middle ring voltage;
V_c : center dot voltage.

This configuration provides the best far-field rejection, equivalent to a BCB sensor, while it produces strong near-field rejection as indicated in Figure 3.

Table 1. Design parameters of the signal conditioning amplifier.

Order	1st order	2nd order	3nd order
Type	Quasi HP	High-pass	Low-pass
Gain	Av=50	Av=2	Av=10
Corner F.	Fc=5Hz	Fc=5Hz	Fc=500Hz
Damping		ζ =0.5	ζ =0.707

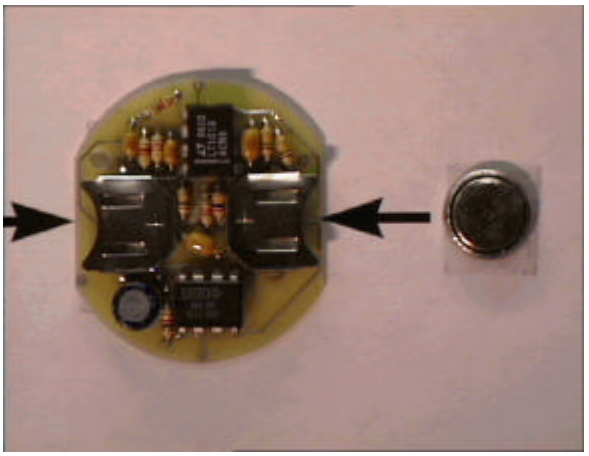

Figure 4. Finished signal conditioning amplifier.

The signal very close to the outer ring of a TCB sensor has a sharper roll-off than the BCB sensor. It yields the best spatial resolution of a wavefront by providing best far- field rejection along with near field rejection. Thus the TCB sensor is most sensitive locally.

The zero crossing between the local maximum and local minimum (as in Fig 1) of the concentric ring sensor's signal indicates the moment when the dipole is moving directly below the center of the sensor where the dot is. It is the instant of this zero crossing that yields the MoA of the moving dipole moving parallel to the plane of the sensor.

High selectivity is achieved because the three closely spaced rings provide spatial differentiation in the immediate vicinity of the sensor, while attenuating both near-field and far-field interference.

The BCB and TCB sensors provide more local information than the unipolar electrodes. The spatial derivative reduces the averaging effect in comparison with a unipolar body surface electrode. Detailed high frequency information is acquired non-invasively with concentric ring electrodes.

We chose the tripolar concentric ring sensor (TCB) for the development of our active sensor. The rings were etched on a printed circuit board with 0.5 mm line thickness for the outer ring with 36mm outer diameter. The contact area between the outer ring and the body surface is 55.76 mm^2. The middle ring's outer diameter is 21.2 mm with a line thickness of 1.2 mm, with 75.40 mm^2 contact area. The dot 5 mm in diameter with 19.63 mm^2 contact area. The contact area of the middle ring electrode is equal to the sum of the other two electrodes. This renders the source impedances of the two input leads to the IA equal, decreasing their mismatch and improving the CMRR.

The radial distances between the inner to the middle electrode and from the middle to the outer ring (6.9 mm) were chosen to be equal, to cancel as much of the common noise as possible for the sake of optimizing the CMR of the TCB electrode.

When the concentric ring sensor is in the magnetic field of a strong power line, it induces a 60 Hz sinusoidal signal that interferes with the signal of interest. The cross-sectional areas of the middle ring and the outer ring are different. The induced 60 Hz interference is greater in the outer ring than in the middle ring. This inductively coupled differential 60 Hz interference can be eliminated by adding a large ground plane on the reverse side of the electrode's double-sided PCB substrate. By grounding this plane, the sensor can be shielded and the interference minimized.

Signal conditioning amplifier with band pass filter

The amplifier mounted on the back of the substrate of the TCB sensor has two major functions: first, to amplify the very small signal detected from the TCB sensor and second, to reject interference. Specifications for a typical active TCB sensor's amplifier are presented in Table 1.

A differential input, quasi high-pass IA, with a unique method for direct coupling to the source, was developed as the first stage of the preamplifier. It provides unity gain for the DC component (1700 mV maximum) generated from the half-cell potentials between the skin and the conductor of the electrode, while amplifying the signal detected from the TCB electrode. The IA (BURR-BROWN: INA118) is operated at low current (0.35 mA) with a low offset voltage (50 µV maximum) and a low input bias current (5 nA maximum). This IA is configured as a high gain amplifier for low-level differential TCB signals, with a high CMRR of 117dB. Its operating voltage is between ± 1.35 V to ± 18 V, with an 8-pin plastic dual-in-line (DIP) housing for battery powered operation. The very high input impedance (10 GΩ) of the IA renders it insensitive to fluctuations of the skin-electrode impedance. Therefore, skin preparation for bioelectric measurements is not necessary.

The differential DC potential appears at the non-inverting input of the IA. This differential DC voltage also appears at the inverting input end of the IA. A single resistor-capacitor set, connected in series, serves as a high- pass filter for both input leads, with a corner frequency of 5 Hz. Therefore, no common signal can be converted into a differential signal, in other words, there is no CMRR degradation! The CMRR, as specified from the manufacturer, can be preserved without the need for complicated circuit design or special sorting of matched components.

The gain of the IA is 50 with a first order quasi-high-pass filter. A second-order active high-pass filter having a gain of 2 with a damping factor of 0.5 is implemented with half of a low-power dual operational amplifier (Linear Technology: LT1013). It rejects the remaining DC offset from the quasi-AC coupled IA. Combining the first order quasi-high-pass filter of the IA and this second order high-pass filter results in a third-order Butterworth high-pass filter with a corner frequency of 5 Hz. High frequency interference is reduced

Figure 5 Finished active sensor with RJ-11 connector.

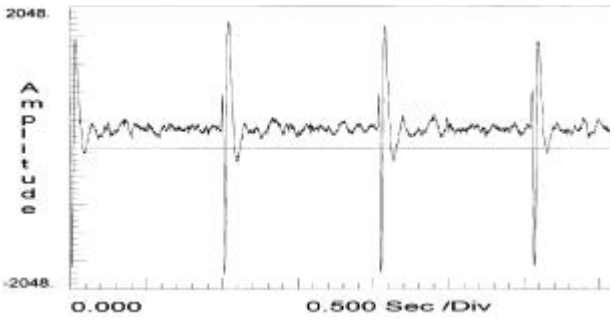

Figure 6 LECG signal with high SNR.

by a second-order Butterworth low-pass active filter with a gain of 10. The amplifier was designed to have a total gain of 1000 with a pass band from 5 Hz to 500 Hz for surface LECG recordings. The output noise level is 0.7 μV_{rms} with two 100 KΩ resistors from the two inputs of the IA to ground.

Figure 4 shows a finished amplifier with the IA and band pass filters for conditioning the LECG signal. The two coin cells can be inserted radially into their cell holders between the substrates of the active sensor; the size of the cell is limited to 12 mm diameter and 1.6 mm to 2.5 mm thickness. Battery capacity ranges from 25 mA-H to 48 mA-H, running the active sensor continuously for 25 to 48 hours.

The TCB sensor with its amplifier is held together with six conductors, these also serve as support posts. Two 8-pins plastic DIP ICs are mounted on the opposite side of the substrate from the TCB electrodes, providing stable, structural integrity. Fig. 5 shows the finished active sensor that combines a TCB electrode and an amplifier.

The TCB active sensor is constructed from a standard circuit layout with an RJ-11 telephone connector. The RJ-11 connector has 50 μm gold plating with a maximum current rating of 1.5 ampere/connection. The amplifier is mounted directly above the electrodes to minimize EMF interference. The high CMR of the concentric ring electrodes, along with the amplifier, result in a very high fidelity active sensor with very high input impedance.

Conclusion and Discussion

Figure 6 depicts an LECG signal from a normal subject recorded approximately at the V2 to V3 ECG location, with its signal to noise ratio (SNR) as high as 150.

These LECG signals, just as the Lead II ECG signal, show high amplitudes for the activity of the ventricles. When the LECGs were recorded simultaneously with the Lead II ECG, with the subject in normal sinus rhythm (NSR), the MoA of the LECG was always in temporal proximity to the Lead II ECG's "R-wave" (L2pk), and typically within 15 ms.

It has often been difficult to have good contact between the rigid active sensor and the body surface of a small subject. A smaller active sensor with 15-mm outer diameter was developed in our lab. The smaller active sensor uses surface-mounted components and a battery on top of the components. It is expected to generate higher quality signals with further clinical applications such as LEEG and Laplacian electromyogram (LEMG) acquisition.

The lighter and smaller active sensor also reduces motion artifacts by forming a better union with the skin surface.

In conclusion, the Laplacian ECG signal obtained from the active concentric ring sensors on the body surface, contains the MoA at a point on the heart, in real time. The sensors may be used without skin preparation and the LECG is obtained without further digital signal processing.

References

[1] Antonioli GE, ed. *Pacemaker leads. Up-date in New Catheters for Endocardial Mapping*, ed. F.e.a. Toscano., Monduzzi: Bologna, Italy. 709-710, 1997.

[2] Fattorusso V, M Thaon, and J Tilmant. " Contribution a l'etude de l'electrocardiogramme precordial", *Acta Cardiol*,. 4: 464-487, 1949.

[3] Fattorusso V. and J. Tilmant." Exploration du champ electrique precordial a l'aide de deux electrodes circulaires, concentriques et rapprochees", *Arch. Mal de Coeur*, 42: 452-455, 1949.

[4] Fye W. " A history of the origin, evolution, and impact of electrocardiography", *American Journal of Cardiology*, 1994. 73(13): 937-949, 1994.

[5] Geselowitz DB, and JE Ferrara. "Is accurate recording of the ECG surface Laplacian feasible? ", *IEEE Trans on BME*, 46(4): 377-381, 1999.

[6] He B. "Theory and applications of body-surface Laplacian ECG mapping", *IEEE Engineering in Medicine and Biology Society*, 17(5): 102-109, 1998.

[7] Hjorth B. "An on-line transformation of EEG scalp potentials into orthogonal source derivations", *Electroenceph. Clin. Neurophysiol.*, 39: 526-530, 1975.

[8] Kaufer M, L Rasquinha, and PP Tarjan. Optimization of multi-ring electrode set. in Ann. International Conf of the IEEE Engineering in Medicine and Biology Society. 1990.

[9] Oosterom, "Av and J Strackee. Computing the lead field of electrodes with axial symmetry", *Medical & Biological Engineering & Computing*, 21: 473-481, 1983.